Pr3+ deactivation effect to Tm3+ at ~1.5 μm emission in Bi4Ge3O12 crystals grown by the micro-pulling-down method

Wen Lu, Jie Xu, Qingsong Song, Kaiting Bian, Jun Guo, Jian Liu, Dongzhen Li, Peng Liu, Chaojin Zhang, Xiaodong Xu, et al.

Pr^{3+} deactivation effect to Tm^{3+} at ~ 1.45 μm emission in $Bi_4Ge_3O_{12}$ crystals grown by the micro-pulling-down method

Wen Lu[a], Jie Xu[a], Qingsong Song[b], Kaiting Bian[a], Jun Guo[a], Jian Liu[b], Dongzhen Li[a], Peng Liu[a], Chaojin Zhang[a], Xiaodong Xu[a,*], Jun Xu[b,*], Kheirreddine Lebbou[c,*]

[a] Jiangsu Key Laboratory of Advanced Laser Materials and Devices, School of Physics and Electronic Engineering, Jiangsu Normal University, Xuzhou 221116, China

[b] School of Physics Science and Engineering, Institute for Advanced Study, Tongji University, Shanghai 200092, China

[c] Institut Lumière Matière, UMR5306 Université Lyon1-CNRS, Université de Lyon, Lyon 69622, Villeurbanne Cedex, France

Corresponding authors:

Email address: xdxu79@jsnu.edu.cn (X. Xu), xujun@mail.shcnc.ac.cn (J. Xu), kheirreddine.lebbou@univ-lyon1.fr (K. Lebbou)

Abstract

Tm^{3+}/Pr^{3+} co-doped $Bi_4Ge_3O_{12}$ (Tm,Pr:BGO) crystals with various Pr^{3+} doping concentration were successfully grown using the micro-pulling-down (μ-PD) method. The use of Pr^{3+} co-doping for deactivating the Tm^{3+} ion at 1.5 μm emission was investigated in the BGO single crystal for the first time. The effect of Pr^{3+} concentration on the spectroscopic properties of Tm,Pr:BGO crystals were demonstrated. In addition, the fluorescence lifetime of Tm^{3+}:$^3F_4$ level of 0.5 at.%, Pr, 2 at.% Tm:BGO crystal is quenched effectively (from 5.64 ms down to 0.36 ms) and the population inversions between Tm^{3+}:$^3H_4$ and $^3F_4$ levels are enhanced to achieve a four-level laser system at 1.5 μm.

Keywords: Tm,Pr:$Bi_4Ge_3O_{12}$, Micro-pulling-down method, Spectroscopic property

1. Introduction

The near-infrared (NIR) emissions around 1.5 μm wavelength have attracted much attention in the past decades for its numerous applications in telecommunication, biomedical systems and remote sensing [1-3]. Tm^{3+} ion is a natural candidate for 1.5 μm laser owing to the $^3H_4 \rightarrow {}^3F_4$ transition. Unfortunately, the self-terminating transition ($^3H_4 \rightarrow {}^3F_4$) of Tm^{3+}ions, namely, the upper level ($^3H_4$), has a shorter lifetime than the lower one ($^3F_4$), almost extinguishing the probability of population inversion for lasing at around the 1.5 μm wavelength. In order to achieve intense Tm^{3+}:$^3H_4 \rightarrow {}^3F_4$ NIR emissions for practical laser operation, co-doping deactivating ions, such as Tb^{3+} [4-9], Ho^{3+} [8]and Eu^{3+} [9,10], is an effective way to depopulate the Tm^{3+}:$^3F_4$ level for population inversion and create a desirable fluorescence lifetime ratio. Moreover, Tm^{3+} lasers emitting at around 1.5 μm have been demonstrated in Tm^{3+}/Ho^{3+} co-doped $YLiF_4$ crystal [11], Tm^{3+}/Tb^{3+} co-doped $YLiF_4$ crystal [12] and Tm^{3+}/Ho^{3+} co-doped tellurite glass microsphere [13]. To the best of our knowledge, there is no report about the use of Pr^{3+} as a deactivated ion of Tm^{3+} for achieving an efficient 1.5 μm fluorescence emission.

$Bi_4Ge_3O_{12}$ (BGO) crystal has some excellent characters as a host of laser gain medium, such as excellent physical and chemical properties [14]. Undoped BGO has broad emission bands which can be converted to narrow bands emission lines when it is doped with rare earth. The crystal belongs to cubic system with the space group of I43d [15]. As it melts congruently, large size single crystals can be obtained by the Bridgman and Czochralski methods. The micro-pulling-down (μ-PD) method can also be used to grow fiber shaped BGO crystals with high quality and good transparency, where the crystals have low thermal strain compared to others growth methods [16-18]. Much research work has been devoted to Nd^{3+} [19, 20], Eu^{3+} [21, 22] doped BGO crystals grown by the μ-PD method as laser gain media. However, Tm^{3+} doped BGO crystal for NIR lasing emission has not been reported yet.

In this work, Tm^{3+}/Pr^{3+} co-doped BGO shaped crystals were successfully grown by the μ-PD method. Pr^{3+} was demonstrated to be an efficient deactivated ion for Tm^{3+} ion to facilitate the Tm^{3+}:$^3H_4 \rightarrow {}^3F_4$ by effective energy transfer from Tm^{3+}:$^3F_4$ level to Pr^{3+}:$^3F_2$ level. Pr^{3+} and Tm^{3+} are attractive dopants because they have many emission lines due to 4f-4f transitions from visible to near infrared wavelengths. The spectroscopic properties of Tm^{3+}/Pr^{3+} co-doped BGO crystals at the 1.5 μm wavelength region for potential NIR laser application was also evaluated. Following our knowledge, not any work with Pr, Tm codoping BGO crystals study luminescence spectra in the NIR region has been investigated.

2. Experiments

The Tm,Pr:BGO crystals were grown using the μ-PD method [23] with the following composition: $Tm_{0.08}Pr_{4x}Bi_{3.92-4x}Ge_4O_{12}$ (x=0, 0.001, 0.002, 0.003, 0.005). Tm_2O_3 (99.999%), Pr_6O_{11} (99.999%), Bi_2O_3 (99.999%) and GeO_2 (99.999%) powders were used as raw materials for crystal growth. The mixture was press into bulks and heated

in the air at 750℃ for 24h. The polycrystalline powders was melted in a platinum crucible, and then the melt was pulled down along the <210> direction through a capillary channel at the bottom of the crucible. The crystals were grown with a pulling rate of 0.3 mm/min in the air atmosphere. As shown in Fig.1, Tm,Pr:BGO cubic structure crystals were obtained with a rough appearance on the outside and present a light yellow color typical to BGO crystal growth from the melt in air atmosphere using Pt crucible. The crystals crystallized from the capillary die of the crucibles were very uniform in diameter according to the measurements performed directly from the fibers with accuracy of about ± 20 μm.

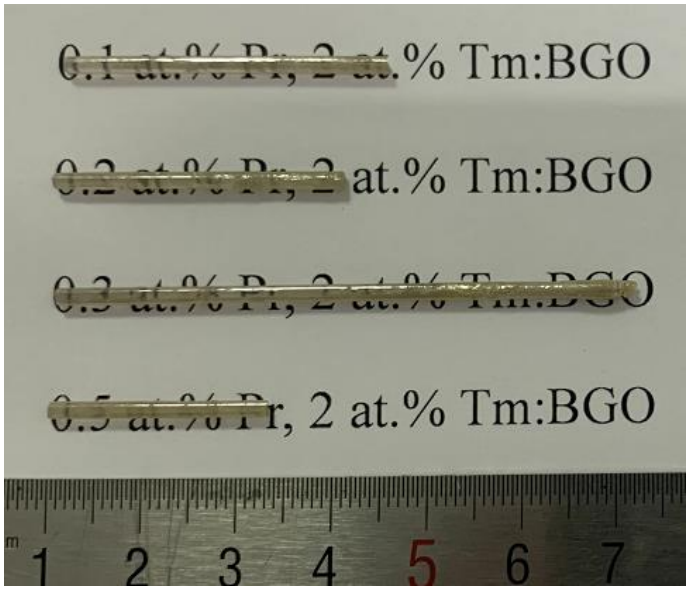

Fig. 1. Photographs of the as-grownTm,Pr codoped BGO crystals

The absorption spectra of Tm,Pr:BGO crystals in the range of 400-2050 nm were measured using a UV–VIS–NIR spectrophotometer (Lambda 1050, Perkins Elmer, U. S. A.). The fluorescence spectra and fluorescence decay curves were recorded by a fluorescence spectrometer (Edinburg Instrument, FLS1000, U. K.) under the excitation of 793 nm. All the measurements were performed at room temperature.

3. Results and discussion

The typical absorption spectra of Tm:BGO and Tm,Pr:BGO crystals are presented in Fig.2. The observed absorption bands are assigned to the transitions from the ground states of Tm^{3+}:$^3H_6$ or Pr^{3+}:$^3H_4$ to the indexed excited ones. Whatever the dopant concentration, no spectral shifts of the absorption spectra were detected. Intensities of the main absorption are mostly similar at room temperature (RT), but relative changes of line intensities are observed. In the range of 760–820 nm, there is one strong absorption band near 792 nm with a full width at half-maximum (FWHM) about 3 nm due to the Tm^{3+}:$^3H_6 \rightarrow {}^3H_4$ transition, which coincides well with the emitting wavelength of high-power AlGaAs laser diodes. Since Pr^{3+} ions do not absorb around

793 nm, they will not reduce the pump efficiency under laser diode excitation.

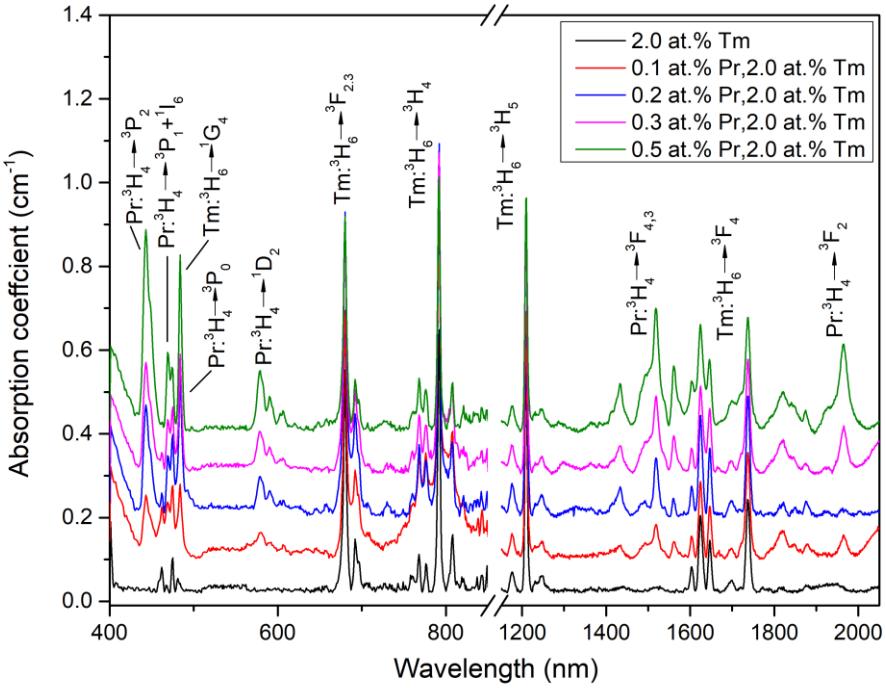

Fig. 2. Room temperature absorption spectra of Tm:BGO and Tm,Pr:BGO crystals

As a function of dopants concentration the NIR and mid-infrared (MIR) emission spectra of Tm:BGO and Tm,Pr:BGO crystals excited at 793 nm are shown in Fig. 3(a) and Fig. 3(b). The NIR emission bands correspond to the Tm^{3+}:$^3H_4 \rightarrow {}^3F_4$ transition and The MIR emission bands are assigned to the Tm^{3+}:$^3F_4 \rightarrow {}^3H_6$ transition. It is clear to see that almost no distinct change in the shape and position of the NIR emission bands were observed at praseodymium concentrations from 0 to 0.5 at.%. The presence of the narrow emissions lines resulting from dopant transition offers a probe of the geometry and crystal field. Moreover, the intensity of the emission bands changed a little. On the contrary, a significant reduction in the MIR emission intensity of the $^3F_4$ level between Tm^{3+} doped and Tm^{3+}/Pr^{3+} co-doped samples, which justifies that Pr^{3+} ions can be used effectively to depopulate the Tm^{3+}:$^3F_4$ level. The intensity of MIR emission decreases with the increase of praseodymium concentration, and the intensity of MIR emission is almost absent when the Pr^{3+} concentration is over 0.3 at.%.

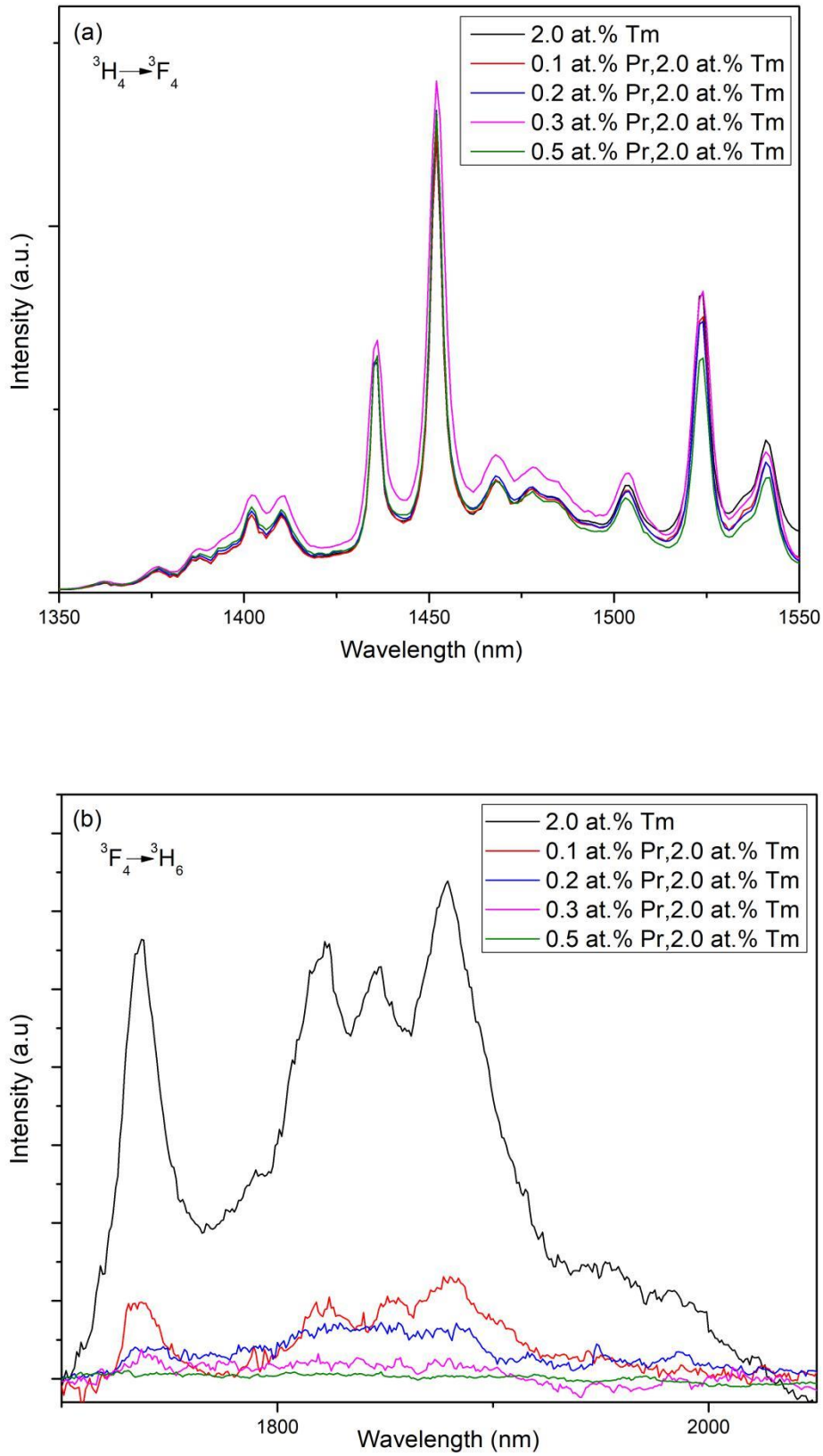

Fig. 3 (a) NIR and (b) MIR fluorescence spectra of Tm:BGO and Tm,Pr:BGO crystals

In order to understand the differences of fluorescence spectra caused by co-doping Pr^{3+}, the energy level scheme of Tm^{3+} and Pr^{3+} is illustrated in Fig. 4. The Tm^{3+} ions were excited from ground state $^3H_6$ to excited state $^3H_4$ through the absorption of 793 nm pumping, and then the ions in the $^3H_4$ level decay radiatively to the $^3F_4$ level with 1.5 μm emission. After that the Tm^{3+} ions in the $^3F_4$ level will decay radiatively to the $^3H_6$ level with emitting 2 μm emission. On the other hand, energy transfer process from $^3F_4$ level of Tm^{3+} to Pr^{3+}: $^3F_4$ (Tm^{3+}) + $^3H_4$ (Pr^{3+}) → $^3H_6$ (Tm^{3+}) + $^3F_2$ (Pr^{3+}) will also happen because of the small energy mismatch between the $^3F_2$ level of Pr^{3+} and the $^3F_4$ level of Tm^{3+}, then the energy will decay very rapidly down to the ground state via multiphonon relaxation. This process would depopulate the $^3F_4$ level of Tm^{3+} and quenching the MIR emission of Tm^{3+}.

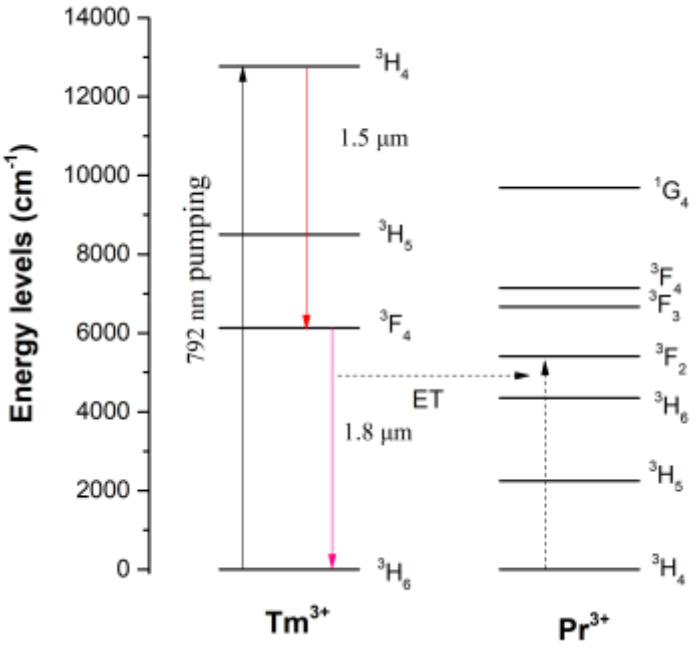

Fig. 4. Simplified energy level diagram of Tm^{3+} and Pr^{3+} co-doped system.

ET: energy transfer from Tm^{3+}:$^3F_4$ level to Pr^{3+}:$^3F_2$ level.

In order to further confirm the energy interaction mechanism, the fluorescence decay curves of Tm^{3+}:$^3H_4$ and $^3F_4$ multiplets of Tm:BGO and Tm,Pr:BGO crystals were measured at 1452 and 1879 nm, as shown in Fig. 5. and Fig. 6. The measured decay curves were fitted with a single exponential function and the fluorescence lifetimes τ are listed in Table 1. It is noticed that the fluorescence lifetime of the $^3H_4$ state (218 μs) is much shorter than that of $^3F_4$ state (5.64 ms) in Tm:BGO crystal due to the cross-relaxation process: $^3H_4$ (Tm^{3+}) + $^3H_6$ (Tm^{3+}) → $^3F_4$ (Tm^{3+}) + $^3F_4$ (Tm^{3+}) [9]. As we know, the lifetime of terminal level $^3F_4$ is too long compared with that of

the emitting level $^3H_4$, which can cause the 1.5 μm laser transition to self-terminate. This is the reason why we grew and examined the decay time of $^3H_4$ and $^3F_4$ level of Tm^{3+}/Pr^{3+}:BGO crystals.

The lifetime of Tm^{3+}:$^3H_4$ level almost keeps constant in Tm,Pr:BGO crystals with the Pr^{3+} doping concentration from 0.1 to 0.3 at.%. Furthermore, when the Pr^{3+} doping concentration is 0.5 at.%, the lifetime of Tm^{3+}:$^3H_4$ level slightly dropes to 160 μs, which is 26.6% shorter compared with that of Tm:BGO crystal (218 μs). The comparable lifetime of Tm^{3+}:$^3H_4$ level in Tm,Pr:BGO crystals suggests that co-doping Pr^{3+} ions has little influence on the upper laser level $^3H_4$. On the contrary, the lifetime of Tm^{3+}:$^3F_4$ level in Tm,Pr:BGO crystals decreases with increasing the doping concentration of praseodymium. The measured lifetime of Tm^{3+}:$^3F_4$ level in 0.5 at.% Pr, 2 at.% BGO crystal is 360 μs, which is 93.6% shorter compared than that of Tm:BGO (5.64 ms), confirming that Pr^{3+} ions can be used as efficient deactivation ions to depopulate the $^3F_4$ level of Tm^{3+} for 1.5 μm emission.

The energy transfer efficiency (η) of Tm^{3+}:$^3F_4$ level to Pr^{3+}:$^3F_2$ level can be evaluated by the following formula [6]:

$$\eta=1-\tau Tm/Pr/\tau Tm \quad (1)$$

where τTm/Pr and τTm are the lifetime of Tm^{3+}:$^3F_4$ level in Tm:BGO crystals with and without Pr^{3+} co-doping, respectively. With increasing the Pr^{3+} doping concentration from 0.1 at.% to 0.5 at.%, the energy transfer efficiency increased from 78.0% to 93.6%, which is much higher than that in Tm,Tb:$GdScO_3$ (35.7% [7]) and Tm,Tb:GLSO (74.4% [6]), indicating that Pr^{3+} ions can efficiently quench the lower laser level of the Tm^{3+}:$^3F_4$. Moreover, the upper laser level ($^3H_4$) to lower laser level ($^3F_4$) fluorescence lifetime ratio in Tm,Pr:BGO crystals are calculated and are also listed in Table 1. The value of 0.5 at.% Pr, 2 at.% BGO crystal is 0.44, which is about eleven times that of the Tm:BGO crystal (0.04). All the results shows that the co-doping of Pr^{3+} ions can lead to an accelerated depletion of population in the laser terminal level $^3F_4$, resulting in lower pump intensities to reach inversion.

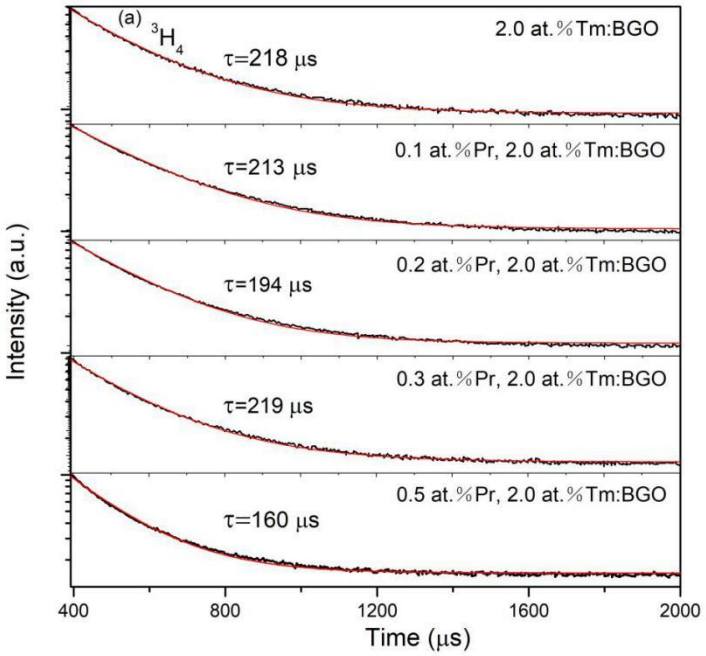

Fig. 5. The decay curves of $^3H_4$ multiplet of Tm:BGO and Tm,Pr:BGO crystals

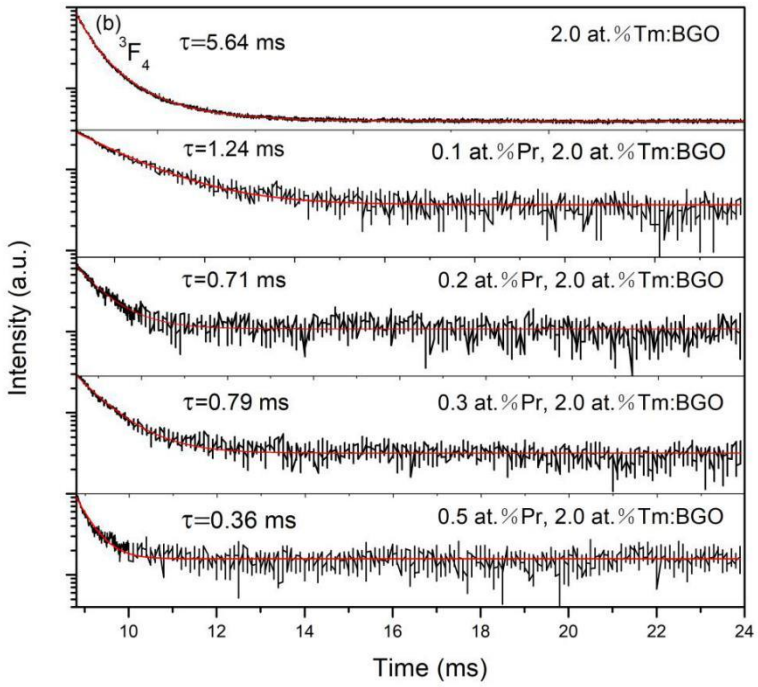

Fig. 6. The decay curves of $^3F_4$ multiplet of Tm:BGO and Tm,Pr:BGO crystals

Table 1. The fluorescence lifetimes of $^3H_4$ and $^3F_4$ levels in Tm:BGO and Tm,Pr:BGO crystals and the energy transfer efficiency from Tm^{3+} to Pr^{3+}

Crystals	$\tau(^3H_4)$	$\tau(^3F_4)$	η(ET)	$\tau(^3H_4)/\tau(^3F_4)$
2 at.% Er:BGO	218 μs	5.64 ms	-	0.04
0.1 at.% Pr, 2 at.% Tm:BGO	213 μs	1.24 ms	78.0%	0.17
0.2 at.% Pr, 2 at.% Tm:BGO	194 μs	0.71 ms	87.4%	0.27
0.3 at.% Pr, 2 at.% Tm:BGO	219 μs	0.79 ms	86.0%	0.28
0.5 at.% Pr, 2 at.% Tm:BGO	160 μs	0.36 ms	93.6%	0.44

4. Conclusion

Tm^{3+}/Pr^{3+} co-doped BGO crystals with various Pr^{3+} doping concentration were successfully grown by the micro-pulling-down method. The BGO accepts Pr^{3+}, Tm^{3+} dopants which they do not make modifications of the stability and the local lattice structure. The efficiency of co-doping Pr^{3+} to deactivate the the laser terminal level $^3F_4$ of the $^3H_4 \rightarrow {}^3F_4$ transition of Tm^{3+} in BGO crystal around 1.5 μm and thus to avoid the bottlenecking effect was demonstrated. It was also demonstrated that the Pr^{3+} doping has little effect on the upper laser level $^3H_4$ of the $^3H_4 \rightarrow {}^3F_4$ transition of Tm^{3+}, which is beneficial to accelerated depletion of population in the laser terminal level $^3F_4$. Moreover, the energy transfer efficiency from Tm^{3+}:$^3F_4$ level to Pr^{3+}:$^3F_2$ level in 0.5 at.% Pr, 2 at.% Tm:BGO crystal was calculated to be 93.6% and the upper laser level ($^3H_4$) to lower laser level ($^3F_4$) fluorescence lifetime ratio (0.44) is about eleven times that of the Tm:BGO crystal (0.04). All of these results indicate that Tm,Pr:BGO crystal could be a promising laser material for 1.5 μm laser applications under the pump of a commercial 793 nm LD.

Funding

National Natural Science Foundation of China (No. 61621001) and “Qinglan Project” of the Young and Middle-aged Academic Leader of Jiangsu College and University.

Disclosures. The authors declare no conflicts of interest.

References

1. P. Loiko , J.L. Doualan , L. Guillemot , R. Moncorge, F. Starecki, A. Benayad, E. Dunina, A. Kornienkom L. Fomicheva, A. Braud, and P. Camy, "Emission properties of Tm^{3+}-doped CaF_2, KY_3F_{10}, $LiYF_4$, $LiLuF_4$ and BaY_2F_8 crystals at 1.5 μm and 2.3 μm," J. Lumin. **225**, 117279 (2020).

2. A. Diening, P. E.-A. Mobert, and G. Huber, "Diode-pumped continuous-wave, Quasi-continuous-wave, and *Q*-switched laser operation of Yb^{3+},Tm^{3+}: $YLiF_4$ at 1.5 and 2.3 μm," J. Appl. Phys. **84**(11), 5900-5904 (1998).

3. R. Allen, L. Esterowitz, and I. Aggarwal, "An Efficient 1.46μm Thulium Fiber Laser via a Cascade Process," IEEE J. Quantum Electron. **29**(2), 303-306 (1993).

4. F.S. Ermeneux, C. Goutaudier, R. Moncorgé, M.T. Cohen-Adad, M. Bettinelli, and E. Cavalli, "Growth and fluorescence properties of Tm^{3+} doped YVO_4 and Y_2O_3 single crystals," Opt. Mater. **8**, 83–90 (1997).

5. W. Ryba-Romanowski, M. Berkowski, B. Viana, and P. Aschehoug, "Relaxation dynamics of excited states of Tm^{3+} in $SrGdGa_3O_7$ crystals activated with Tm^{3+} and Tm^{3+}+Tb^{3+}," Appl. Phys. B **64**, 525-529 (1997).

6. P. Zhang, X. Huang, R. Wang, Z. Li, H. Yin, S. Zhu, Z. Chen, and Y. Hang, "Enhanced 1.4 μm emissions of Tm^{3+} via Tb^{3+} deactivation in $(Gd_{0.5}Lu_{0.5})_2SiO_5$ crystal," Opt. Mater. Express. **8**(3), 668–675(2018).

7. Q. Li, J. Dong, Q. Wang, H. Zhao, Y. Xue, H. Tang, X. Xu, and J. Xu, "Growth and spectroscopic properties of Tm^{3+} and Tb^{3+} co-doped $GdScO_3$ crystal," J. Lumin. **230**, 117681 (2021).

8. M. Bettinelli, F.S. Ermeneux, R. Moncorgé, and E. Cavalli, "Fluorescence dynamics of YVO_4:Tm^{3+}, YVO_4:Tm^{3+},Tb^{3+} and YVO_4:Tm^{3+},Ho^{3+} crystals," J. Phys.: Condens. Matter **10**, 8207-8215 (1998).

9. A. Braud, S. Girard, J.L. Doualan, and R. Moncorgé, "Spectroscopy and Fluorescence Dynamics of (Tm^{3+}, Tb^{3+}) and (Tm^{3+}, Eu^{3+}) Doped $LiYF_4$ Single Crystals for 1.5 μm Laser Operation," IEEE J. Quantun Electron. **34**(11), 2246-2255 (1998).

10. R. Lisiecki, W. Ryba-Romanowski, and T. Lukasiewics, "Relaxation of excited states of $Tm^{3+}$and Tm^{3+}–Eu^{3+}energy transfer in YVO_4 crystal," Appl. Phys. B **83**, 255-259 (2006).

11. R.C. Stoneman, and L. Esterowitz, "Continuous-wave 1.50-μm thulium cascade laser," Opt. Lett. **16** (4), 232-234 (1991).

12. G. H. Rosenblatt, R. C. Stoneman, and L. Esterowitz, "Diode-Pumped Room-Temperature cw 1.45-μm Tm,Tb:YLF laser, Advanced Solid State Lasers," Optical Society of America, Salt Lake City, Utah, 1990: p. DPL8.

13. A.Li, W.Li, M. Zhang, Y. Zhang, S. Wang, A. Yang, Z. Yang, and E. Lewis, G. Brambilla, and P. Wang, "Tm^{3+}-Ho^{3+} codoped tellurite glass microsphere laser in the 1.47 μm wavelength region," Opt. Lett. **44**(3), 511-513 (2019).

14. P.A. Williams, A.H. Rose, K.S. Lee, D.C. Conrad, G.W. Day, and P.D. Hale, "Optical, thermo-optic, electro-optic, and photoelastic properties of bismuth germanate ($Bi_4Ge_3O_{12}$)," Appl. Opt. **35**(19), 3562-3569 (1996).

15. S.A.S. Farias, and M.V. Lalic, "The local structure around the Nd impurity incorporated

into the $Bi_4Ge_3O_{12}$ crystal matrix: An ab initio study," Solid. State Commun. **150**, 1241-1244 (2010).

16. J.B. Shim, J.H. Lee, A. Yoshikawa, M. Nikl, D.H. Yoon, and T. Fukuda, "Growth of $Bi_4Ge_3O_{12}$ single crystal by the micro-pulling-down method from bismuth rich composition," J. Cryst. Growth **243**, 157-163 (2002).

17. V. Chani, K. Lebbou, B. Hautefeuille, O. Tillement, and J.-M. Fourmigue, "Evaporation induced diameter control in fiber crystal growth by micro-pulling-down technique: $Bi_4Ge_3O_{12}$," Cryst. Res. Technol. **41**, 972-978 (2006).

18. H. Farhi, S. Belkahla, K. Lebbou, and C. Dujardin, "BGO fibers growth by μ-pulling down technique and study of light propagation," Phys. Procedia **2**, 819-825 (2009).

19. N. Li, Y. Xue, D. Wang, B. Liu, C. Guo, Q. Song, X. Xu, J. Liu, D. Li, J. Xu, Z. Xu, and J. Xu, "Spectroscopic properties of Eu:$Bi_4Ge_3O_{12}$ single crystal grown by the micro-pulling down method," J. Lumin. **208**, 208-212 (2019).

20. Y. Lin, Q. Wu, S. Wang, A. Wu, L. Su, L. Zheng, J. Chen, Z. Qin, G. Xie, X. Xu, Q.Song, and Q. Hang, "Growth and laser properties of Nd^{3+}-doped $Bi_4Ge_3O_{12}$ single-crystal fiber," Opt. Lett. **43**(6), 1219-1221 (2018).

21. J.B. Shim, A. Yoshikawa, M. Nikl, and T. Fukuda, "Eu^{3+} doped $Bi_4Ge_3O_{12}$ fiber crystals grown by the by the micro-pulling down method," J. Cryst. Growth **245**, 67-72 (2002).

22. N. Li, Y. Xue, D. Wang, B. Liu, C. Guo, Q. Song, X. Xu, J. Liu, D. Li, J. Xu, Z. Xu, and J. Xu, "Optical properties of Nd:$Bi_4Ge_3O_{12}$ crystals grown by the micro-pulling down method," J. Lumin. **206**, 412-416 (2019).

23. Q. Song, X. Xu, J. Liu, X. Bu, D. Li, P. Liu, Y. Wang, J. Xu, and K. Lebbou, "Structure and white LED properties of Ce-doped YAG-Al_2O_3 eutectics grown by the micro-pulling-down method," CrystEngComm, **21**, 4545-4550 (2019).